Reptation Dynamics of Semirigid Polymers in Porous Media

Iwao Teraoka,*,† Kenneth H. Langley,‡ and Frank E. Karasz†

Polymer Science and Engineering Department and Department of Physics and Astronomy, University of Massachusetts, Amherst, Massachusetts 01003

Received November 13, 1991; Revised Manuscript Received July 23, 1992

ABSTRACT: A theory of the dynamics of a semirigid polymer molecule in a porous medium is formulated on the basis of the reptation theory. The porous medium is assumed to be made up of a network of hollow cylinders of uniform radius, a model approximating the situation in controlled pore glasses. When the pores confine a long semirigid chain with a persistence length at least comparable to the pore radius, the chain takes an extended conformation, wiggling around the center line (primitive path) of the tube formed by the solid pore walls; this result is confirmed through a computer simulation. Because of the rigidity of the pore walls, the tube and the primitive path have the conformation of a wormlike chain with a persistence length (usually longer than that of the semirigid chain) determined by the pore structure. The computer simulation comparing chains of the same extension in the pore network and identical concentration in the fluid surrounding the porous material shows that a semirigid chain with a persistence length intermediate between the pore radius and the persistence length of the primitive path will be present in the largest concentration within the pore. When the primitive path moves its center of mass in the porous medium, the motion of the semirigid chain is restricted to travel along the pore and the tube. We notice that the restricted motion fulfills the basic assumption of the reptation theory of Doi and Edwards for entangled linear flexible chains but that the conformation of the primitive path is different here. Applying the formulation of the reptation theory to the dynamics of the primitive path, we obtain the long-time diffusion constant of the semirigid polymer as a function of the chain geometry and the pore geometry. For the short-time behavior of the chain dynamics in the pore network, we employ the normal-mode analysis for an isolated wormlike chain developed by Aragón and Pecora. Combining the two results, we obtain the mean-square displacement of monomers on a sufficiently long semirigid polymer chain as t^{α}, where $\alpha \cong 1/4$ for the short-time wiggling motion inside the pore, $\alpha \cong 1$ for the translational motion along a pore within one pore branch, $\alpha \cong 1/2$ for the intermediate time region where the reptation mode along the tube dominates, and $\alpha = 1$ for the long-time diffusion beyond the tube dimension. The intermediate region, however, is not distinctly observed unless the polymer chain is extremely long.

Introduction

Transport properties of diffusants such as small particles[1] and polymer molecules[2-4] inside inert porous media filled with a solvent have been increasingly studied in recent years. The broad interest is a direct consequence of a wide range of applications of the porous media, for example, to size-exclusion chromatography, membrane filtration, and enhanced oil recovery. Moreover, a porous medium composed of inert pore walls is an ideal model system for examining the behavior of the diffusants encountering random geometrical and hydrodynamic hindrance without undergoing any specific surface interaction.[5]

Static properties of polymer molecules in the porous medium such as a free energy increase[6-8] and chain conformation[9-13] have been of intense interest, in particular, when the chain dimension is comparable to or much larger than the pore size. A change of the chain conformation in a straight cylindrical pore has been studied theoretically for chains with a persistence length much smaller[7] and much larger[14] than the pore diameter. The dynamics have been worked out for flexible linear chain polymers in a single pore.[15] The convection effect that occurs when there is a macroscopic flow of the solution inside the single pore has been treated by Davidson and Deen.[16] Sahimi and Jue[17] and Muthukumar and Baumgärtner[18,19] treated the diffusion of the chains in a three-dimensional network of pores. However, their networks consisted of a regular array of pores.

We present a theory for the dynamics of semirigid chain molecules in porous glasses, a typical porous medium. We pay attention to the detailed structure in the three dimensions of the porous glasses. The glass portion and the vacant space form an infinitely extending bicontinuous structure in three dimensions. The pore space can be approximated by an assembly of hollow cylinders of radius R_P and length L_N connected to other cylinders at both ends. There are distributions in R_P and L_N, reflecting the randomness of the porous network.

In such a porous medium, a semirigid chain with persistence length larger than R_P adopts a conformation extending along the pore. The chain is confined in a tubelike space constructed by the surrounding pore walls. Chain diffusion occurs as the chain ends penetrate unexplored branches of the pore network. We can treat these dynamics over a long distance in a formulation similar to the reptation theory[20] originally developed for entangled linear flexible polymers in concentrated solutions and melts.

The development in this paper is as follows. First, we consider statics, i.e., the dimensions and conformation of a semirigid chain in a straight cylindrical pore. We will also discuss the partition coefficient of the chain between solutions in the interior and the exterior of the pore. Then we discuss the statics of the semirigid chain in a random network of pores in three dimensions. Definitions of the tube and the primitive path are given here together with their statistical properties that are different from those for entangled flexible polymers. The dynamics will be discussed in subsequent sections. First, we formulate the motion of the primitive path in analogy to the reptation theory.[20] We calculate the mean-square displacement of a point on the primitive path in the pore network and obtain the long-time diffusion constant as a function of the chain length, pore size, and pore structure. To treat

† Polymer Science and Engineering Department.
‡ Department of Physics and Astronomy.

0024-9297/92/2225-6106$03.00/0

the short-time motion of the real chain confined in the pore network, we employ the normal-mode analysis for a wormlike chain developed by Aragón and Pecora.[21]

Statics of Polymer Chains in a Cylindrical Pore

As a model for the conformation of a linear chain polymer in a free solution, we employ a wormlike chain model[22] with a persistence length L_P and a contour length L_C. In this model, the mean-square end-to-end distance R_{F0}^2 of the chain in a dilute solution is expressed as

$$R_{F0}^2 = 2L_C L_P g(L_C/L_P) \quad (1)$$

where

$$g(x) \equiv 1 - \frac{1}{x}[1 - \exp(-x)] \quad \text{with } x = L_C/L_P \quad (2)$$

In this section we study static properties of the wormlike chain in a straight cylindrical pore. When a long linear chain of some rigidity is placed inside a straight cylindrical pore of radius R_P, the chain will adopt a conformation extending along the pore space. Let R_F be the root mean square of the end-to-end distance of the chain in the cylindrical pore; then $R_F > R_{F0}$.

The chain dimension R_F for a sufficiently long chain ($R_{F0} \gg R_P$) confined in a cylindrical pore has been expressed in the two cases of limiting chain rigidities. For an ideal flexible chain, i.e., without an excluded-volume effect, the confinement does not alter the chain dimension in the direction parallel to the pore:[15]

$$R_F/L_C \sim (a/L_C)^{1/2} \quad (3)$$

where a is the monomer size. As the chain rigidity increases, the conformation becomes more extended parallel to the pore. Odijk obtained,[14] for a sufficiently rigid chain

$$R_F/L_C = 1 - (3/16)^{1/3}(R_P/L_P)^{2/3} \quad (4)$$

by introducing "deflection length" $(R_P^2 L_P)^{1/3}$ at which the persistent chain is deflected by pore walls. It is interesting to note that a flexible chain with an excluded-volume effect is extended along the pore, i.e., $R_F/L_C \sim (a/R_P)^{2/3}$, as suggested by Daoud and de Gennes.[7]

Partitioning of polymer chains between a porous medium and a bulk solution in equilibrium with the pore has been studied intensively. Size-exclusion chromatography directly utilizes this property. The partition coefficient p_I is defined as the ratio of the polymer concentration inside the pores of the medium to that in the bulk solution. The concentration of the chains in the bulk solution is assumed to be much smaller than the overlap concentration. If we denote by ΔF an increase in the free energy of the chain inside the porous medium with respect to that in the bulk solution, the $p_I = \exp(-\Delta F/k_B T)$, where k_B is the Boltzmann constant and T is the absolute temperature. The partition coefficient was also calculated for the two limiting chain rigidities. Casassa and Tagami[23,24] obtained p_I for an ideal flexible chain as

$$p_I \cong \exp[-\alpha_1(R_F/R_P)^2] \quad (5)$$

where α_1 is a numerical constant. For a rigid chain, Odijk gave[14]

$$p_I \cong \exp\left[-\alpha_2 \frac{L_C}{(D_P^2 L_P)^{1/3}} \log\left(\frac{L_P}{D_P}\right)\right] \quad (6)$$

where α_2 is a second numerical constant and D_P is the pore diameter ($D_P = 2R_P$).

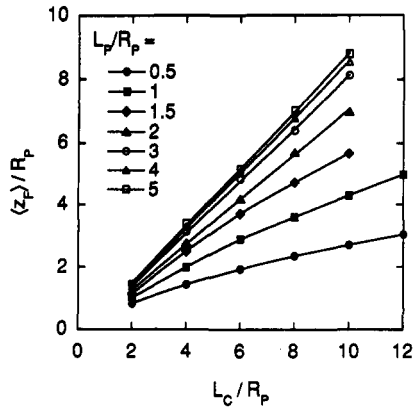

Figure 1. Average of chain extension parallel to the pore, $\langle z_F \rangle$, versus the contour length L_C of a wormlike chain with persistence length L_P confined in a straight cylindrical pore of radius R_P. All lengths are normalized to R_P. Only the symbols are produced by the computer simulation; the solid lines merely guide the eye.

To estimate the chain extension along the pore and the partition coefficient for finite chain rigidity, we performed a computer simulation. A wormlike chain was generated on the basis of a model of jointed rods (N rods in total), with a difference $\Delta\mathbf{u}$ in the direction vectors of adjacent rod segments being distributed with a probability density $\exp(-\Delta u^2/2\sigma^2)$, where $\sigma^2 = L_C/NL_P$. There is no correlation between $\Delta\mathbf{u}$ on different joints. When $N \gg 1$, this model gives rise to a chain in free space with the end-to-end distance given by eq 1. A straight cylindrical pore with radius R_P was placed with the axis extending in the z direction. A semirigid chain was generated inside the cylinder in a run by first selecting a random position on a cross section of the cylinder with a plane perpendicular to its axis. Then, the first segment was oriented at random, followed by the rest of the segments created with the probability density given above. Once a newly jointed rod segment emerged from the cylinder, the run was discarded. After a sufficient number of chains were created inside the pore, the mean-square end-to-end distance R_F^2, the mean length $\langle z_F \rangle$ of the chain extension z_F in the z direction, and its variance $\langle \Delta z_F^2 \rangle$ were calculated. The chain extension z_F is here defined by $z_F \equiv \max_{0 \le i \le N}(z_i) - \min_{0 \le i \le N}(z_i)$, where z_i is the z component of the position coordinate of the ith joint.

Figure 1 is a plot of $\langle z_F \rangle$ against L_C for several values of L_P. All lengths are normalized to R_P. As the chain becomes more rigid, $\langle z_F \rangle$ tends to be proportional to L_C with a proportionality coefficient approaching unity, a relation consistent with eq 4 with $\langle z_F \rangle \cong R_F$.

The fluctuation in z_F becomes smaller as the chain rigidity increases. It is estimated as $\langle \Delta z_F^2 \rangle / \langle z_F \rangle^2 \sim (R_P/L_P)^{4/3}$ for a sufficiently rigid and long chain, following the discussion given by Odijk.[14] Therefore, just as the chain contraction factor $1 - \langle z_F \rangle / L_C$ decreases as $(R_P/L_P)^{2/3}$ with increasing chain rigidity, the fluctuation in the chain extension decreases as $\langle \Delta z_F^2 \rangle^{1/2} / \langle z_F \rangle \sim (R_P/L_P)^{2/3}$. This tendency was also verified in the computer simulation. In the discussion that follows, we neglect the fluctuation in z_F and regard $z_F \cong \langle z_F \rangle \cong R_F$.

In the computer simulation for the chain conformation, the partition coefficient p_I was also calculated as a probability of a whole chain being generated within the cylindrical pore. When p_I is plotted against the reduced contour length L_C/R_P for different values of L_P/R_P (iso-L_P line), then p_I decreases as L_C/R_P increases, and the iso-L_P line with a smaller L_P lies above that with a larger L_P in the parameter range examined. A more flexible chain has a larger partition coefficient if we compare chains of the

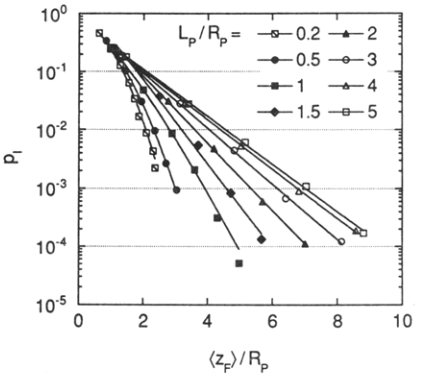

Figure 2. Partition coefficient between the interior and the exterior of a straight cylindrical pore, p_I, for a wormlike chain, plotted as a function of the average of chain extension $\langle z_F \rangle$. The persistence length is L_P, the contour length L_C, and the pore radius R_P. All lengths are normalized to R_P. Only the symbols are produced by the computer simulation; the lines are to guide the eye along the symbols obtained for the same values of L_P.

same contour length L_C. The situation, however, is different, when chains of the same dimension in a given cylindrical pore are compared. In Figure 2, p_I is plotted against $\langle z_F \rangle / R_P$ for different chain rigidities, L_P/R_P. The iso-L_P lines nearly overlap for $L_P/R_P < 0.2$, a characteristic of a flexible chain. As L_P increases and exceeds R_P, the iso-L_P line moves upward in the figure. Comparing chain molecules of the same $\langle z_F \rangle$ in the pore network, we see that p_I is larger for the more rigid chains. The difference becomes even more prominent as $\langle z_F \rangle / R_P$ increases. This tendency can be explained as follows: As the chain rigidity increases, the geometrical constraint has a smaller effect on the number of conformations available to the chain in the cylindrical pore. Once the conformations are selected that extend the chain in the z direction at the initial stage of the segment generation in the simulation, chain rigidity facilitates the added segments being generated within the cylindrical pore. As the chain rigidity decreases, this property diminishes. Thus for a flexible chain, adding new segments to the chain end within the cylinder to increase $\langle z_F \rangle$ is not entropically easier than generating the same number of segments from the first step inside the cylinder.

It is also observed in the figure that the difference in the entropy ($-k_B \ln p_I$) increases as a linear function of $\langle z_F \rangle / R_P$ when L_P/R_P is large, whereas it is a higher order function of $\langle z_F \rangle / R_P$ when L_P/R_P is not large. This result is consistent with eqs 5 and 6.

Semirigid Chains in a Network of Pores

In a three-dimensional network of pores, the space available for the chain is not straight but is curved over lengths larger than L_N. The conformation of the chain has to change to fit the curved space. The wormlike chain is confined in a tubelike region consisting of z_F/L_N ($\cong R_F/L_N$) cylinders of radius R_P and length L_N, as illustrated in Figure 3. The statistics for the wiggling of the chain around the centerline of the tube are the same for straight and curved pores. Thus, the contour length of the tube (the one measured along the pore centerline; this is different from the chain contour length L_C) is R_F. The end-to-end distance in the three-dimensional network of pores is smaller than R_F.

On a short time scale, the chain undergoes local wiggling motions within the tube. Long-time motion is limited to movements of the chain along the curved tube. Because the tube is not infinitely long, a portion of the tube will

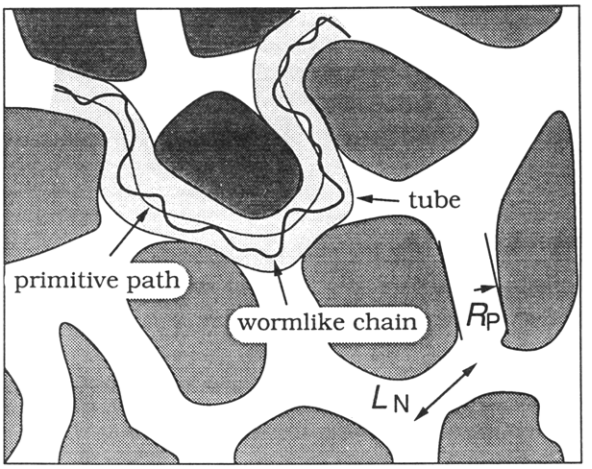

Figure 3. Schematic representation of a semirigid chain confined in a porous medium. Darker shading represents the space occupied by solid material, for example, silica in the controlled pore glass. Because the pore walls are solid and the chain has a persistence length at least comparable to the pore radius, the chain has an extended conformation. We can define a tube (lighter shading) as a series of concatenated pore branches in which the chain is confined. The centerline of the tube (the primitive path) has the conformation of a wormlike chain with a persistence length determined by the geometrical structure of the pores.

be created when the chain end moves forward, comes to a pore junction, and chooses any of the other pore branches.

We call the centerline of the tube the "primitive path". The primitive path has a contour length R_F and the conformation of the trapped chain itself but represents the average of short-time lateral motions (mostly wiggling). The concepts of a "tube" and a "primitive path" have been widely used[15,20] to explain complicated but challenging features we encounter in the dynamics of entangled linear flexible polymers in concentrated solutions and melts. We note that one of the major motivations for studying the dynamics of chain molecules in porous media is to examine the reptation dynamics, because, compared with concentrated solutions and melts, the tube and primitive path in the pore network can be optimally defined with solid pore walls, which provide the basic assumption of the tube in the reptation theory.

The tube in reptation theory for entangled linear flexible chains is modeled as a Rouse chain with a step length different from that of the flexible polymer chain. Note, however, that the tube and the primitive path defined for the porous media have a nonzero persistence length because the pore walls are rigid and the pores are locally straight at least over the length R_P. The crudest approximation for the conformation of the primitive path would be a sequence of straight segments of length L_N ($\gg R_P$). However, actual porous materials such as controlled pore glasses have distributions in R_P and L_N. It seems more natural to approximate the conformation of the primitive path by a continuously bending wormlike chain with a persistence length $(2\lambda)^{-1}$ rather than by a sequence of segments. The persistence length is larger than R_P and should be close to L_N. The persistence length $(2\lambda)^{-1}$ characterizes the pore structure, in particular, the pore connectivity, although it was defined for a tube confining the semirigid chain of another persistence length. To model the primitive path by the conformation analogous to a wormlike chain has the advantage that the model is mathematically simple, with only one parameter, $(2\lambda)^{-1}$. When the contour length of the primitive path R_F is in the range $R_F \ll (2\lambda)^{-1}$ or $(2\lambda)^{-1} \ll R_F$, the conformations of the

primitive path are the same as the conformation of a straight cylinder or that of a flexible chain, respectively. The mean-square end-to-end distance of the primitive path in the porous network is $(R_F/\lambda)g(2\lambda R_F)$ by analogy with eq 1.

Here we consider the partition coefficient of a semirigid chain in a three-dimensional network of pores. We demonstrated in the computer simulation that, comparing chain molecules of the same R_F, chain extension along a cylindrical pore, the free energy increase is larger for more flexible chains. As shown by the iso-L_P lines in Figure 2, the increase is dominant for a chain with $L_P \lesssim R_P$, if the chain is sufficiently long. The same applies to a curved pore. The partition coefficient is the same as that in the straight pore once the tube is fixed. Note, however, that branching in the pore network allows the tube to adopt different conformations, which is not the case for the straight pore. Thus the partitioning coefficient for a semirigid chain in the pore network should be multiplied by the number of different conformations available for the tube. This number depends on the structure of the pore network alone and not on the rigidity of the polymer molecule, as long as the polymer has some flexibility to fit in the curved space.

When the pore is curvilinear in space, a mismatch between rigid but curved pore walls and a stiff chain that favors a straight conformation can produce an increase in the (bending) free energy. The increase will be dominant for a chain with persistence length $L_P \gtrsim (2\lambda)^{-1}$, if the chain is long enough. Disorder in the porous media will produce pore branches that have a large curvature and are almost inaccessible to a very rigid chain. These voids will make the dynamic behavior of the chain quite different in nature.

Combining these two factors, we find that a minimum in the free energy increase for a chain of variable flexibility but of the same R_F, chain extension along the pore, occurs for a chain with L_P in the range $R_P \lesssim L_P \lesssim (2\lambda)^{-1}$. Such a chain can enter the pore network most easily, because it is least affected by the partitioning of chain molecules between a location inside the pore network and one in the bulk solution. This conclusion means that experiments for pores immersed in solutions containing the polymer molecules are most readily performed for systems in which $R_P \lesssim L_P \lesssim (2\lambda)^{-1}$. For example, in a light scattering experiment, the signal intensity is proportional to the number of polymer molecules in the scattering volume in the pore network. Note also that a tube for the semirigid chain with $R_P \lesssim L_P \lesssim (2\lambda)^{-1}$ has a well-defined contour length with a small fluctuation.

Therefore, the theory of chain dynamics we develop in the following discussion is designed to explain the behavior of a chain with a persistence length L_P in the range $R_P \lesssim L_P \lesssim (2\lambda)^{-1}$. When this condition is satisfied, the picture for the motion of the semirigid chain in the pore network is as follows: A wormlike chain with a persistence length L_P makes wriggling and reptating motions in a wormlike tube with a persistence length $(2\lambda)^{-1}$. When the real chain moves along the tube, so does the primitive path defined as the centerline of the tube. The ends of the primitive path are allowed to choose their directions with the restriction that the ever-changing primitive path also have the conformation of a wormlike chain of the same persistence length. The rest of the primitive path moves along its own contour, following its leading end. Thus, the real chain (and the primitive path) can move its center of mass in the three-dimensional pore network.

Reptation Dynamics of the Primitive Path

In this section we consider the dynamics of the primitive path along its contour R_F in the three-dimensional network of pores. We follow the formulation employed by Doi and Edwards[20] to treat the dynamics of entangled flexible polymers. Let us denote by D_L a long-time one-dimensional diffusion constant of the primitive path inside a straight cylindrical pore of radius R_P. When the condition $R_P \lesssim L_P \lesssim (2\lambda)^{-1}$ is satisfied, D_L is equal to the diffusion constant of the semirigid chain along the tube contour in the pore network. Because of confinement and a hydrodynamic interaction between the highly confined chain and the pore wall, the longitudinal diffusion constant D_L is much reduced relative to the translational diffusion constant in free solution. It will be a complicated function of R_P, L_P, and L_C. For a sufficiently long chain with $R_F \gg R_P$, $D_L \propto L_C^{-1} \propto R_F^{-1}$ holds. We need not go into the details here regarding D_L, which we treat as a given quantity.

Let us define the two-point mean-square displacement $\phi(s,s';t)$ of the primitive path in three dimensions as

$$\phi(s,s';t) \equiv \langle [\mathbf{r}(s,t) - \mathbf{r}(s',0)]^2 \rangle \tag{7}$$

where s and s' are contours on the primitive path ($0 \le s, s' \le R_F$), and $\mathbf{r}(s,t)$ denotes the position of a point on the path at the contour s at time t. The average $\langle \bullet \rangle$ is taken with respect to position and conformation of the primitive path at times 0 and t. Since the primitive path diffuses along its contour with diffusion constant D_L, $\phi(s,s';t)$ satisfies[20]

$$\frac{\partial \phi}{\partial t} = D_L \frac{\partial^2 \phi}{\partial s^2} \tag{8}$$

The initial condition is given by

$$\phi(s,s';0) = \frac{|s-s'|}{\lambda} g(2\lambda|s-s'|) \tag{9}$$

The boundary conditions can be derived as follows. Differentiating eq 7 with respect to s at $s = R_F$, we obtain

$$\begin{aligned} \frac{\partial}{\partial s}\phi(s,s';t)|_{s=R_F} &= 2\langle \mathbf{u}(R_F,t)\cdot[\mathbf{r}(R_F,t) - \mathbf{r}(s',0)] \rangle \\ &= 2\langle \mathbf{u}(R_F,t)\cdot[\mathbf{r}(R_F,t) - \mathbf{r}(s',t)] \rangle + \\ &\quad 2\langle \mathbf{u}(R_F,t)\cdot[\mathbf{r}(s',t) - \mathbf{r}(s',0)] \rangle \end{aligned} \tag{10}$$

where $\mathbf{u}(s,t) \equiv \partial \mathbf{r}(s,t)\partial s$ is a tangential vector of the primitive path at s. The second term vanishes because there is always a component giving $-[\mathbf{r}(s',t) - \mathbf{r}(s',0)]$ for the same $\mathbf{u}(R_F,t)$ in the configurational spaces of the initial and the final (at time t) chain positions and conformations. Then eq 10 leads to

$$\begin{aligned} \frac{\partial}{\partial s}\phi(s,s';t)|_{s=R_F} &= \frac{\partial}{\partial s}\langle [\mathbf{r}(s,t) - \mathbf{r}(s',t)]^2 \rangle|_{s=R_F} \\ &= \frac{1}{\lambda}[1 - \exp(-2\lambda(R_F - s'))] \end{aligned} \tag{11}$$

Likewise

$$\frac{\partial}{\partial s}\phi(s,s';t)|_{s=0} = -\frac{1}{\lambda}[1 - \exp(-2\lambda s')] \tag{12}$$

The solution of eq 8 that satisfies the initial conditions

and the boundary conditions is given by

$$\phi(s,s';t) = \frac{|s-s'|}{\lambda} g(2\lambda|s-s'|) + \frac{2D_L}{\lambda R_F} g(2\lambda R_F)\, t + 16R_F^2 \sum_{p=1}^{\infty} A_p(\lambda R_F) \cos\frac{p\pi s}{R_F} \cos\frac{p\pi s'}{R_F}\left[1 - \exp\left(-\frac{p^2 t}{\tau_d}\right)\right] \quad (13)$$

where $A_p(z)$ is a nonnegative function defined by

$$A_p(z) \equiv \frac{1}{(p\pi)^2} \frac{z}{4z^2 + (p\pi)^2}\left[1 - \frac{4z(1-(-1)^p e^{-2z})}{4z^2 + (p\pi)^2}\right] \quad (14)$$

and

$$\tau_d \equiv R_F^2/\pi^2 D_L \quad (15)$$

is the disengagement time proportional to R_F^3 when $R_F \gg R_P$. The first term of the right-hand side of eq 13 is just the initial distribution, which vanishes for $s = s'$. The second term becomes dominant for large t. The third term is responsible for the short-time behavior of the primitive path, arising from local motion along its contour.

It is interesting to determine the mean-square displacement of the primitive path $\langle\phi(s,s;t)\rangle$ in the two limiting cases of the primitive path conformation, where

$$\langle\phi(s,s;t)\rangle \equiv \frac{1}{R_F}\int_0^{R_F} \phi(s,s;t)\, ds \quad (16)$$

Note that we are concerned here with a spatial displacement of a point on the contour, so that $s' = s$. In the coil limit of the primitive path ($\lambda R_F \to \infty$), $g(2\lambda R_F) = 1$ and $A_p(z) = (4z)^{-1}(p\pi)^{-2}$ for $z = \lambda R_F$. Then, eq 13 reproduces the reptation dynamics of entangled flexible chains by the identity $a = \lambda^{-1}$, where a is the step length of the primitive chain.[20] The other extreme is the rod limit ($\lambda R_F \to 0$), in which we have $(2D_L/\lambda R_F)g(2\lambda R_F) = 2D_L$ and $A_p(z) = z(p\pi)^{-4}$. Then the motion of the primitive path is nothing but translational diffusion with a one-dimensional diffusion constant D_L inside the straight pore cylinder. Note the difference in the power dependence of $A_p(z)$ on p. The higher-order mode (larger p) is less dominant in eq 13 for a straighter primitive path.

Now we proceed to obtain the expressions for the mean-square displacement $\langle\phi(s,s;t)\rangle$ of a point on the primitive path in the short time scale $t \ll \tau_N \equiv (\lambda^2 D_L)^{-1}$ and in the long time scale $t \gg \tau_d$. Here, τ_N is the time needed for the primitive path to diffuse a distance over which the pore is regarded as straight. First, in the long time scale, the mean-square displacement is diffusive. The long-time diffusion constant D is given by

$$D \equiv \lim_{t\to\infty} \frac{\langle\phi(s,s;t)\rangle}{6t} = \frac{1}{3} D_L \frac{g(2\lambda R_F)}{\lambda R_F} \quad (17)$$

The factor $^1/_3$ derives from the one-dimensional nature of the diffusion along the pore, and the factor $g(2\lambda R_F)/\lambda R_F$ comes from the geometrical constraint of the tube winding in space. It decreases monotonically from 1 to 0 as λR_F increases from 0; i.e., the primitive path approaches the conformation of a flexible chain. When the chain is sufficiently long ($\lambda R_F \gg 1$), the expression is simply

$$D = \frac{1}{3}\frac{D_L}{\lambda R_F} \quad (18)$$

Since $D_L \propto R_F^{-1}$ for a chain with $\lambda R_F \gg 1$, $D \propto R_F^{-2} \propto L_C^{-2}$ holds, an outcome that reproduces the result of the reptation theory for entangled flexible chains.

In the short time scale, on the other hand, $1 - \exp(-p^2 t/\tau_d)$ in eq 13 can be replaced by $p^2 t/\tau_d$. By substituting $\cos^2(p\pi s/R_F)$ with its average $^1/_2$ and calculating the sum, we arrive at $\langle\phi(s,s;t)\rangle = 2D_L t$, an outcome showing that the motion of the primitive path is also diffusive in the short time scale.

Figure 4 is a log–log plot of $\langle\phi(s,s;t)\rangle/R_F^2$ against $D_L t/R_F^2 = t/(\pi^2\tau_d)$ for $\lambda R_F = 10^{-1}$, 10^0, 10^1, 10^2, 10^3, and 10^4. The slope is nearly 1 in the two limiting time regimes $t \ll \tau_N$ and $t \gg \pi^2\tau_d$. As λR_F increases, the lower boundary τ_N shifts to the left in Figure 4 in terms of the normalized time $D_L t/R_F^2$. The two boundaries correspond to $\langle\phi(s,s;t)\rangle \ll \lambda^{-2}$ ($\simeq$mean-square distance between adjacent pore junctions in the branch-junction picture of the pore) and $\langle\phi(s,s;t)\rangle \gg (R_F/\lambda)g(2\lambda R_F)$ (=mean-square end-to-end distance of the primitive path in the pore network), respectively. Between them, the slope is less than unity but larger than $^1/_2$. We can observe a slope close to $^1/_2$ only when $\lambda R_F \gtrsim 100$. The slope of $^1/_2$ in the intermediate time range is characteristic of reptation dynamics,[20] i.e., one-dimensional Brownian motion on a path created by a random walk. Indeed, we get $\phi(s,s;t) \sim t^{1/2}$ by first taking the asymptotic form of $A_p(\lambda R_F)$ for $\lambda R_F \to \infty$ and then calculating the sum in eq 13 by replacing it with an integral. Note that, unless $\lambda R_F \gtrsim 100$, the slope is larger than $^1/_2$, and there is no well-defined intermediate range.

The correlation function $\psi(s,s';t)$ of the tangential vector $\mathbf{u}(s,t)$ can be calculated. It is defined by

$$\psi(s,s';t) \equiv \langle \mathbf{u}(s,t)\cdot\mathbf{u}(s',0)\rangle \quad (19)$$

which is calculated from eq 7 as

$$\psi(s,s';t) = -\frac{1}{2}\frac{\partial^2}{\partial s\, \partial s'}\phi(s,s';t) = 8\sum_{p=1}^{\infty}(p\pi)^2 A_p(\lambda R_F) \sin\frac{p\pi s}{R_F}\sin\frac{p\pi s'}{R_F} \times \exp\left(-\frac{p^2 t}{\tau_d}\right) \quad (20)$$

From this, we can also obtain the correlation function $C(t)$ of the end-to-end vector $\mathbf{r}(R_F,t) - \mathbf{r}(0,t)$ of the primitive path as

$$C(t) = \langle[\mathbf{r}(R_F,t) - \mathbf{r}(0,t)]\cdot[\mathbf{r}(R_F,0) - \mathbf{r}(0,0)]\rangle = \int_0^{R_F} ds \int_0^{R_F} ds'\, \psi(s,s';t) = 32R_F^2 \sum_{p:\,\text{odd}}^{\infty} A_p(\lambda R_F) \exp(-p^2 t/\tau_d) \quad (21)$$

Bending Motions for Short Time Scales

For the long time scale, the mean-square displacement of the primitive path $\langle\phi(s,s;t)\rangle$ is equal to the monomer mean-square displacement $\langle\Delta\mathbf{r}^2\rangle_m$ of the real chain. For the short time scale, however, $\langle\Delta\mathbf{r}^2\rangle_m$ can be different from $\langle\phi(s,s;t)\rangle$. The bending motions, especially those of shorter wavelengths and higher frequencies, become dominant.

Aragón and Pecora[21] presented a normal-mode analysis for the dynamics of an isolated wormlike chain in a dilute solution. Noting that the stretching motion is faster by several orders of magnitude than the bending motion, they started with a Langevin equation for the dynamics of the chain with an elasticity bending constant $k_B T L_P/2$ and an infinite elastic constant of stretching. Following their

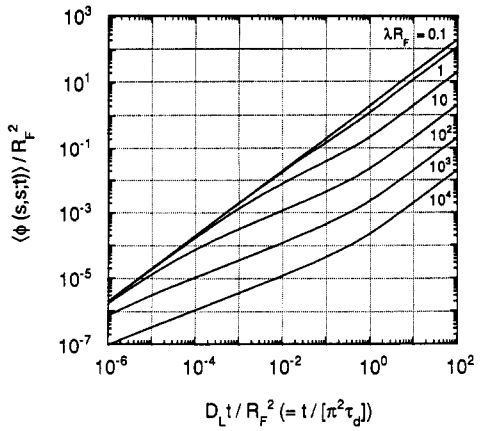

Figure 4. log–log plot of $\langle\phi(s,s;t)\rangle/R_F^2$, the normalized mean-square displacement of a point on the primitive path at time t, as a function of normalized time $D_L t/R_F^2 = t/(\pi^2\tau_d)$, where D_L is the one-dimensional diffusion constant of the chain in the pore, and τ_d is the disengagement time given as a function of the chain length. The plots are given for different chain lengths λR_F = 10^{-1}, 10^0, 10^1, 10^2, 10^3, and 10^4.

notations and applying the analysis to the monomer mean-square displacement, we obtain

$$\langle\Delta\mathbf{r}^2\rangle_m = 2L_C^2\sum_{l=0}^{\infty} d_{ll}\left(\frac{L_C}{2L_P}\right)\left[1-\exp\left(-\frac{\lambda_l t}{\zeta}\right)\right] \quad (22)$$

where λ_l is the eigenvalue of the lth normal mode and ζ is a friction constant per unit chain length. For the definitions of $d_{ll}(y)$, see Aragón and Pecora.[21] The eigenvalue is given by[21]

$$\lambda_l \cong L_P k_B T\left[\frac{\pi}{2}\frac{2l+1}{L_C}\right]^4 \quad (23)$$

The lth normal mode is characterized by a wavelength $L_C/(l+1/2)$. For $l \gg 1$, Aragón[25] calculated $d_{ll}(y)$ as

$$d_{ll}(y) = \frac{y}{\pi^2 l^2(y^2+\pi^2 l^2/4)} \quad (24)$$

When the semirigid chain is confined in a cylindrical pore, the geometrical constraint suppresses normal modes with characteristic wavelengths larger than R_P. However, for a short time scale such as $\langle\Delta\mathbf{r}^2\rangle_m \lesssim R_P^2$, the wormlike chain moves just like one in a free solution. Then the higher-order modes dominate and the discrete sum in eq 22 can be replaced by an integral, which yields

$$\langle\Delta\mathbf{r}^2\rangle_m = \frac{4L_P^2}{\pi} f\left(\frac{t}{\tau_C}\right) \quad (25)$$

where $\tau_C \equiv L_P^3/D_0 L_C$, and

$$f(x) \equiv \int_0^\infty \frac{1-\exp(-xu^4)}{u^2(1+u^2)}\,du \quad (26)$$

Here, the diffusion constant D_0 in a free solution is related to the friction coefficient by $D_0 = k_B T/L_C\zeta$. We substitute $u^2(1+u^2)$ in eq 26 with u^q, where $2 \le q \le 4$. The limiting values correspond to $L_C/L_P \to \infty$ (coil) and $L_C/L_P \to 0$ (rod), respectively. Then, we get

$$\langle\Delta\mathbf{r}^2\rangle_m = \frac{4L_P^2}{\pi}\frac{\Gamma((5-q)/4)}{q-1}(t/\tau_C)^{(q-1)/4} \quad (27)$$

Since $L_C/L_P > 1$ from the assumption and $q \cong 2$, $\langle\Delta\mathbf{r}^2\rangle_m \sim t^\alpha$ with $\alpha \cong 1/4$. The upper limit τ_W of the time range for this short-time behavior is derived from $\langle\Delta\mathbf{r}^2\rangle_m \lesssim R_P^2$ as

$$t \lesssim \tau_W \equiv \tau_C\left(\frac{\pi}{4}\right)^4\left(\frac{R_P}{L_P}\right)^8 \quad (28)$$

Note that the short-time motion of a Rouse chain gives $\alpha = 1/2$.[20] The power $\alpha \cong 1/4$ comes from $\lambda_l \propto l^4$ in the normal-mode analysis for a semirigid chain (see eq 23), whereas in the Rouse chain, $\lambda_l \propto l^2$. As noted by Aragón and Pecora,[21] the coil limit of the wormlike chain shows short-time behavior different from that of the Rouse chain.

Combining the results for the primitive path and the real chain, we can summarize the dynamic behavior of the sufficiently long semirigid chain in the network of a pore as $\langle\Delta\mathbf{r}^2\rangle_m \sim t^\alpha$, where (1) $\alpha \cong 1/4$ ($t \lesssim \tau_W$), wriggling motions of short wavelength; (2) $\alpha \cong 1$ ($\tau_W \lesssim t \lesssim \tau_N$), translational motion along a pore within one pore branch; (3) $\alpha \cong 1/2$ ($\tau_N \lesssim t \lesssim \tau_d$), reptating motion along a winding tube; and (4) $\alpha = 1$ ($\tau_d \lesssim t$), diffusion over a distance larger than the tube dimension. Domain (2) will be embedded in domains (1) and (3) unless $R_P \ll L_N \approx \lambda^{-1}$. The time domain (3) will not be clearly observed when λR_F is not so large and therefore $\tau_W \ll \tau_d$ is not satisfied. Then we will see a gradual increase of the power index from 1/4 to 1.

Concluding Remarks

Unlike the tube encapsulating an entangled linear polymer in concentrated solutions and melts, the tube constructed by inert pore walls in the network of pores corresponds exactly to the assumption of a solid, immobile constraint in the reptation theory. There is no other mode available for the overall diffusion of the chain than translation along the tube. The only complication of the system is the small partition coefficient of the polymer chains between the interior of the pore network and the outside (in the bulk solution). However, when we compare linear chains of the same dimensions in the pore network, we find that the coefficient is larger for a more rigid chain, unless the chain is extremely rigid and cannot bend to conform to the curved pore network. This larger partition coefficient is one of the advantages of exploring the diffusion of semirigid polymer chains in a solid confining geometry in order to study the mechanism of molecular motions for the overall diffusion of the chains. Another advantage is a smaller fluctuation in the tube length, compared with that of the entangled linear flexible chains in melts. In the reptation theory for entangled flexible chains, a fluctuation in the tube length and the Gaussian nature of the tube conformation are often confused.

To our knowledge, no experimental data have been obtained for the dynamics of semirigid polymers in porous materials. We are currently experimenting with poly(hexyl isocyanate) in controlled pore glass. We are using the technique of dynamic light scattering to detect the motion of polymer molecules in the porous glass filled with solvent. Because of the poor contrast of the polymer against the solvent (which must be index-matched to the porous glass), the intensity of light scattered by the polymer molecules is weak compared with that scattered by the glass; therefore, data accumulation takes considerable time. Results will be published later.

In our formulation, we neglected the fluctuation in the tube length R_F. This assumption is not valid unless the chain is sufficiently rigid and long. When either $L_P > R_P$ or $L_C \gg R_P$ is not satisfied, there is another mechanism for the overall diffusion of the chains. By contracting and stretching R_F (not L_C), we can cause the chain end to

explore new branches in the pore network; this mechanism increases the mobility of the chain. Such movement is more likely to occur with more flexible or shorter chains. Then, the apparent power dependence of the diffusion constant on the chain length L_C can be sharper than that predicted in eq 18.

Our formulation can be applied to other systems. One example is a semirigid chain molecule in a dense gel.[26] When the persistence length L_P of the chain is larger than the mean node distance L_N of the gel, the motion of the chain is limited to sliding along its contour except for the chain head and the tail and the short-time wriggling motions. In this system, the primitive path is the chain itself, the tube contour R_F is equal to the chain contour L_C, and the persistence length of the tube $(2\lambda)^{-1}$ is equal to that of the chain L_P. The results obtained here will apply with these alterations.

Acknowledgment. We thank S. R. Aragón for making available a preprint of his paper. This work was in part supported by the Air Force Office of Scientific Research Grant No. 91-001.

References and Notes

(1) Dullien, F. A. L. *Porous Media: Fluid Transport and Pore Structure*; Academic Press: New York, 1979.
(2) Bishop, M. T.; Langley, K. H.; Karasz, F. E. *Macromolecules* **1989**, *22*, 1220.
(3) Easwar, N.; Langley, K. H.; Karasz, F. E. *Macromolecules* **1990**, *23*, 738.
(4) Guo, Y.; Langley, K. H.; Karasz, F. E. *Macromolecules* **1990**, *23*, 2022.
(5) Drake, J. M.; Klafter, J. *Phys. Today* **1990**, *43*, No. 5, 46.
(6) Giddings, J. C.; Kucera, E.; Russel, C. P.; Myers, M. N. *J. Phys. Chem.* **1968**, *72*, 4397.
(7) Daoud, M.; de Gennes, P.-G. *J. Phys. (Paris)* **1977**, *38*, 85.
(8) Doi, M. *J. Chem. Soc., Faradey Trans. 2* **1974**, *55*, 1720.
(9) Edwards, S. F.; Muthukumar, M. *J. Chem. Phys.* **1988**, *89*, 2435.
(10) Muthukumar, M. *J. Chem. Phys.* **1989**, *90*, 4594.
(11) Honeycutt, J. D.; Thirumalai, D.; Klimov, D. K. *J. Phys. A* **1989**, *22*, L169.
(12) Honeycutt, J. D.; Thirumalai, D. *J. Chem. Phys.* **1989**, *90*, 4542.
(13) Honeycutt, J. D.; Thirumalai, D. *J. Chem. Phys.* **1990**, *93*, 6851.
(14) Odijk, T. *Macromolecules* **1983**, *16*, 1340.
(15) de Gennes, P.-G. *Scaling Concepts in Polymer Physics*; Cornell University Press: Ithaca, NY, 1979.
(16) Davidson, M. G.; Deen, W. M. *J. Membr. Sci.* **1988**, *35*, 167.
(17) Sahimi, M.; Jue, V. L. *Phys. Rev. Lett.* **1989**, *62*, 629.
(18) Muthukumar, M.; Baumgärtner, A. *Macromolecules* **1989**, *22*, 1941.
(19) Muthukumar, M.; Baumgärtner, A. *Macromolecules* **1989**, *22*, 1937.
(20) Doi, M.; Edwards, S. F. *The Theory of Polymer Dynamics*; Clarendon Press: Oxford, 1986.
(21) Aragón, S. R.; Pecora, R. *Macromolecules* **1985**, *18*, 1868.
(22) Tsvetkov, V. N. *Rigid-Chain Polymers*; Plenum: New York, 1989.
(23) Casassa, E. F. *J. Polym. Sci., Poly. Lett. Ed.* **1967**, *5*, 773.
(24) Casassa, E. F.; Tagami, Y. *Macromolecules* **1969**, *2*, 14.
(25) Aragón, S. R. *Macromolecules* **1991**, *24*, 3451.
(26) Slater, G. W., private communication.